Hydroxyhydroquinone, a by-product of coffee bean roasting, increases intracellular Ca^{2+} concentration in rat thymic lymphocytes

Risa Kamae[1], Shoko Nojima[2], Kenji Akiyoshi[3], Shoki Setsu[3], Sari Honda[2], Toshiya Masuda[2], Yasuo Oyama[1,3,4]

[1] Faculty of Integrated Arts and Sciences, Tokushima University, Tokushima 770-8502, Japan

[2] Graduate School of Human Life Science, Osaka City University, Osaka 558-8585, Japan

[3] Graduate School of Integrated Arts and Sciences, Tokushima University, Tokushima 770-8502, Japan

[4] Faculty of Bioscience and Bioindustry, Tokushima University, Tokushima 770-8513, Japan

*Corresponding author: Yasuo Oyama, Ph.D.

E-mail: oyamay@tokushima-u.ac.jp Tel: 81-88-656-7256

Abstract

Hydroxyhydroquinone (HHQ) is generated during coffee bean roasting. A cup of coffee contains 0.1–1.7 mg of HHQ. The actions of HHQ on mammalian DNA were examined because HHQ is a metabolite of benzene, which causes leukemia. Currently, information on the cellular actions of HHQ is limited. We examined the effects of sublethal levels of HHQ on the concentration of intracellular Ca^{2+} in rat thymic lymphocytes by using a flow cytometric technique with fluorescent probes. HHQ at 10 μM or more significantly elevated intracellular Ca^{2+} levels by increasing the membrane permeability of divalent cations, resulting in hyperpolarization via the activation of Ca^{2+}-dependent K^{+} channels. HHQ-induced changes in the intracellular Ca^{2+} concentration and membrane potential may affect the cell functions of lymphocytes. HHQ-reduced coffee may be preferable in order to avoid the possible adverse effects of HHQ.

Keywords: hydroxyhydroquinone; by-product; coffee; cytotoxicity; lymphocytes; calcium

1. Introduction

During coffee bean roasting, hydroxyhydroquinone (HHQ) is generated from carbohydrates, amino acids, and free or chlorogenic acid-bound quinic acid moieties (Müller et al., 2006). HHQ generates hydrogen peroxide in a neutral solution by consuming dissolved oxygen (Hiramoto et al., 2001). HHQ reacts with 2-furfurylthiol, a compound that smells like coffee, and other odor-active thiols, such as methanethiol (Müller and Hofmann, 2007). HHQ interferes with the chlorogenic acid-induced restoration of endothelial function in spontaneously hypertensive rats (Suzuki et al., 2008). HHQ is a benzene metabolite and since benzene causes leukemia, the effects of benzene and its metabolites on mammalian DNA were examined. Benzene metabolites induce oxidative stress, which causes the formation of DNA adducts (Lévay and Bodell, 1992; Hedli et al., 1996), breakage of DNA strands (Lee and Garner, 1991), inhibition of nuclear DNA synthesis or DNA replication (Schwartz et al., 1985; Lee et al., 1989), and DNA damage (Pellack-Walker and Blumer, 1986). HHQ at concentrations of 50 μM or more is supposed to induce adverse actions on mammalian DNA from above studies. The information regarding the bioactive effects of HHQ seem to be biased toward the aspects of DNA damage and induction of oxidative stress. A cup of coffee typically contains 0.1–1.7 mg of HHQ (Ochiai et al., 2008). Since coffee is commonly consumed worldwide, a large amount of HHQ could be ingested per day. Thus, it is necessary to elucidate the basic information that predicts the various bioactive effects of HHQ. In the present study, we used flow cytometric techniques and rat thymocytes to determine the sublethal concentrations of HHQ and examined the effects of sublethal levels of HHQ on cellular parameters to characterize the action of HHQ. We used thymocytes in our in vitro studies because they can be prepared without any enzymatic treatment for dissociation and their cell membranes remain intact. In addition, the process of cell death (apoptosis, necrosis, and autophagy) is commonly studied using lymphocytes.

2. Materials and methods

2.1. Chemicals

HHQ and furaneol (DHF) were purchased from Tokyo Chemical Industry Co., Ltd. (Tokyo, Japan). The purities of HHQ and DHF were 99.9 % and 98.4 %, respectively. Pyrogalol (PGR) was obtained from Wako Pure Chemicals (Osaka, Japan) and its purity was 99.9 %. DHF and PGR are also contained in coffee. These compounds were used as references.

Propidium iodide, annexin V-FITC, hydroethidine, 5-chloromethylfluorescein diacetate (5-CMF-DA), and bis-(1,3-dibutylbarbituric acid)trimethine oxonol (Oxinol) were obtained from Molecular Probes Inc., Invitrogen (Eugene, OR, USA). Zn^{2+} chelators, diethylenetriamine-N,N,N′,N″,N″-pentaacetic acid (DTPA) for extracellular Zn^{2+} and N,N,N′,N′-tetrakis(2-pyridylmethyl)ethylenediamine (TPEN) for intracellular Zn^{2+}, were obtained from Dojin Chemical Laboratory (Kumamoto, Japan). Other chemicals were obtained from Wako Pure Chemicals unless mentioned.

2.2. Animals and cell preparation

This study was approved by the Committee for Animal Experiments at the University of Tokushima (No. 05279).

The cell suspension was prepared as previously reported (Chikahisa et al., 1996; Matsui et al., 2010). In brief, thymus glands dissected from ether-anesthetized rats were sliced under cold conditions (2–4 °C). The slices were triturated in chilled Tyrode's solution to dissociate the thymocytes. The cell-containing solution was then passed through a 56-μm diameter mesh to prepare the cell suspension. The cell suspension was incubated at 36–37 °C for 1 h before the experiment. Importantly, the zinc concentration in the cell suspension was 216.9 ± 14.4 nM (Sakanashi et al., 2009). The cell suspension contained trace amounts of zinc derived from the cell preparation.

Various concentrations of HHQ (10–100 mM in 2 μL dimethyl sulfoxide) were added to the cell suspensions (2 mL per test tube) and incubated at 36–37 °C for 2–4 h. A sample from each cell suspension (100 μL) was analyzed using flow cytometry to assess the

fungicide-induced changes in cellular parameters. Data acquisition from 2×10^3 cells or 2.5×10^3 cells required 10–15 s.

2.3. Fluorescence measurements of cellular parameters

The methods for measuring cellular and membrane parameters using a flow cytometer equipped with an argon laser (CytoACE-150; JASCO, Tokyo, Japan) and fluorescent probes were similar to those previously described (Chikahisa et al., 1996; Matsui et al., 2010). The fluorescence was analyzed using JASCO software (Version 3.06; JASCO, Tokyo, Japan). There was no fluorescence from the reagents used in the study, except for the fluorescent probes, under our experimental conditions.

To assess cell mortality, propidium iodide was added to the cell suspensions to a final concentration of 5 μM. Because propidium stains dead cells, the measurement of propidium fluorescence from cells provided information on mortality. The fluorescence was measured 2 min after the application of propidium iodide by a flow cytometer. The excitation wavelength used for propidium was 488 nm, and the emission was detected at 600 ± 20 nm.

Exposure of phosphatidylserine on the outer surface of cell membranes, a phenomenon during the early stage of apoptosis, was detected using annexin V-FITC (Koopman et al., 1994). The cells were incubated with annexin V-FITC (10 μl/mL) for 30 min before the measurement.

Fluo-3-AM was used to monitor changes in the intracellular Ca^{2+} concentration (Kao et al., 1989). The cells were incubated with 500 nM Fluo-3-AM for 60 min prior to any fluorescence measurements. The excitation wavelength used for Fluo-3 was 488 nm, and the emission was detected at 530 ± 20 nm.

FluoZin-3-AM (500 nM) was added to the cell suspension to assess the change in the intracellular Zn^{2+} concentration (Gee et al., 2002). Cells were incubated with FluoZin-3-AM for 50–60 min before the application of the drug. FluoZin-3 fluorescence was measured from the cells that were not stained with propidium iodide (living cells with intact membranes). The

excitation wavelength used for FluoZin-3 was 488 nm, and the emission was detected at 530 ± 20 nm.

Change in the membrane potential of the rat thymocytes was estimated with 300 nM Oxonol (Wilson and Chused, 1985). The excitation wavelength for Oxonol was 488 nm, while the emission was detected at 530 ± 20 nm.

2.4. Statistical analysis and presentation

Statistical analyses were performed through an analysis of variance, with post hoc Tukey's multivariate analysis. P-values less than 0.05 were considered statistically significant. In the results, values (columns and bars in figures) are expressed as the mean and the standard deviation of 4–8 samples. Each experiment was repeated three times unless noted otherwise.

3. Results

3.1. Effects of HHQ, pyrogalol (PRG), and furaneol (DHF) on cell mortality

The cells were respectively incubated with HHQ (10–100 μM), PRG (10–100 μM), and DHF (100 μM) for 4 h. PRG at 100 μM slightly but significantly increased the cell mortality (Fig. 1).

(Figure 1 near here)

3.2. Effects of HHQ, PRG, and DHF on side scatter

As shown in Fig. 2A, the incubation of cells with 100 μM HHQ for 4 h changed the cytogram (forward scatter versus side scatter). HHQ at 100 μM increased the side scatter. The concentration-dependent changes in the side scatter induced by HHQ (10–100 μM), PRG (10–100 μM), and DHF (100 μM) are summarized in Fig. 2B. Significant increases in the intensity of the side scatter were observed in the cases of HHQ (10–100 μM) and PRG (100 μM). It is noted that HHQ augmented the side scatter without increasing the cell mortality.

(Figure 2 near here)

3.3. HHQ-induced change in the cell population, classified using propidium iodide and Annexin

V-FITC

The cytogram is shown in Fig. 3A (propidium fluorescence versus FITC fluorescence). Incubation with 100 μM HHQ for 4 h decreased the population of intact living cells (area N) and increased that of annexin V-positive living cells (area A) without affecting those of dead cells (areas P and AP). The percentage changes in the population induced by 100 μM HHQ are shown in Fig. 3B.

(Figure 3 near here)

3.4. HHQ-induced increase in intracellular Ca^{2+} concentration

Similar to those previously mentioned, changes in the side scatter were observed, including the drug-induced disturbance of intracellular Ca^{2+} homeostasis (Kinazaki et al., 2009). Therefore, to confirm whether HHQ increases the intracellular Ca^{2+} concentration, HHQ-induced changes in the mean intensity of Fluo-3 fluorescence were examined. As shown in Fig. 4, HHQ at 10–50 μM significantly increased the intensity of Fluo-3 fluorescence in a concentration-dependent manner, suggesting that HHQ induced an increase in intracellular Ca^{2+} levels. The removal of extracellular Ca^{2+} by 2 mM EDTA in nominal Ca^{2+}-free Tyrode's solution completely abolished the HHQ-induced augmentation of Fluo-3 fluorescence (Fig. 5A). This indicates the dependence on extracellular Ca^{2+}. Therefore, there was a possibility that HHQ non-specifically increased membrane permeability. To test this possibility, the effect of 2 mM $MnCl_2$ on the augmentation of Fluo-3 fluorescence induced by HHQ was examined. As shown in Fig. 5B, the Fluo-3 fluorescence of cells treated with 50 μM HHQ significantly reduced when 2 mM $MnCl_2$ was added, indicating the permeation of Mn^{2+}.

(Figures 4 and 5 near here)

3.5. Disturbance of HHQ-induced augmentation of Fluo-3 fluorescence by Zn^{2+}

Normal cell suspensions contained trace amount of Zn^{2+} (Sakanashi et al., 2009). TPEN, a chelator of intracellular Zn^{2+}, at 10 μM augmented the HHQ-induced increase in the intensity of Fluo-3 fluorescence (Fig. 6A). The result suggests that the removal of intracellular Zn^{2+}

increases the intensity of Fluo-3 in the cells treated with HHQ. Thus, there was a possibility that HHQ also increased the intracellular Zn^{2+} concentration. To assess whether HHQ increases the intracellular Zn^{2+} concentration, the change in the intensity of FluoZin-3 fluorescence induced by 50 μM HHQ was examined in the absence or presence of TPEN. As shown in Fig. 6B, the augmentation of FluoZin-3 by HHQ was completely diminished by TPEN. The result indicates that HHQ induced an increase in the intracellular Zn^{2+} concentration.

(Figure 6 near here)

3.6. HHQ-induced change in the intensity of Oxonol fluorescence

The increase in the intracellular Ca^{2+} concentration induces hyperpolarization because the membranes of rat thymocytes possess Ca^{2+}-dependent K^+ channels (Wilson and Chused, 1985). If HHQ increases the intracellular Ca^{2+} concentration, it would attenuate the intensity of Oxonol fluorescence, a parameter of membrane potential. The incubation of cells with 50 μM HHQ for 2 h decreased the intensity of Oxonol fluorescence (Fig. 7). This suggests that HHQ induced hyperpolarization.

(Figure 7 near here)

4. Discussion

4.1. HHQ-induced increase in the intracellular Ca^{2+} concentration

It is unlikely that HHQ non-specifically increases membrane ionic permeability, resulting in the increase in intracellular Ca^{2+} concentration. If HHQ induces a non-specific increase in membrane ionic permeability, the membranes would be depolarized. However, HHQ hyperpolarized the membranes of rat thymocytes (Fig. 7). The increase in intracellular Ca^{2+} levels induced by HHQ causes the activation of K^+ channels, resulting in hyperpolarization, since the cells possess Ca^{2+}-dependent K^+ channels (Wilson and Chused, 1985). Mn^{2+} appears to pass through the membranes of cells treated with HHQ because the Fluo-3 fluorescence was quenched in the presence of external Mn^{2+} (Fig. 5B). Therefore, HHQ is assumed to increase the

membrane permeability of divalent metal cations. It is also unlikely that HHQ releases Ca^{2+} from the intracellular Ca^{2+} store, which would result in the elevation of the intracellular Ca^{2+} level. The removal of external Ca^{2+} completely diminished the HHQ-induced increase in the intracellular Ca^{2+} concentration (Fig. 5A), suggesting that there was no release of intracellular Ca^{2+}. Thus, it is concluded that HHQ at sublethal concentrations (10–50 μM) significantly elevates intracellular Ca^{2+} levels via increasing membrane Ca^{2+} permeability, under the in vitro conditions used in this study.

4.2. Toxicological implication

Sublethal concentrations of HHQ increased the intensity of the side scatter (Fig. 2). HHQ was assumed to change intracellular circumstances because the side scatter is proportional to cell granularity or internal complexity. HHQ elevated intracellular Ca^{2+} levels (Fig. 4). The increase in the intracellular Ca^{2+} concentration is an essential triggering signal for the activation of T cells by antigens and other stimuli that cross-link the T-cell antigen receptor (Robert et al., 2011; Fracchia et al., 2013). HHQ may disturb intracellular Ca^{2+} signaling in lymphocytes, possibly disrupting the function of immune cells. Furthermore, if high concentrations of intracellular Ca^{2+} are in the presence of HHQ, this phenomenon would trigger processes associated with cell death, such as necrosis, apoptosis, and autophagy (Harr and Distelhorst, 2010). In rat thymocytes, as shown in Fig. 3, the incubation with 100 μM HHQ increased the population of living cells with exposed phosphatidylserine, a phenomenon during early stage of apoptosis. Same phenomenon was observed in the cells treated with A23187, a calcium ionophore (Nishimura et al., 2006; Sakanashi et al., 2008). Excessive increase in intracellular Ca^{2+} concentration by HHQ is though to trigger apoptosis.

A cup of coffee typically contains 0.1–1.7 mg of HHQ (Ochiai et al., 2008). Since coffee is commonly consumed worldwide, certain individuals may intake large amounts of HHQ per day. Currently, there is no information regarding blood HHQ levels after consuming coffee because the pharmacokinetics of HHQ have not been elucidated. HHQ at 10 μM (1.26 mg/L) is

assumed to elevate the intracellular Ca^{2+} levels of lymphocytes, resulting in hyperpolarization. HHQ-induced changes in intracellular Ca^{2+} levels and membrane potentials may affect the cell function of lymphocytes. Although it is impossible to achieve micromolar HHQ concentrations in the usual consumption of coffee without accumulation, HHQ-reduced coffee may be preferable in order to avoid any possible adverse effects of HHQ.

Conflict of interest

All authors affirm that there are no conflicts of interest to declare.

Acknowledgements

This study was supported by Grant-in-Aids for Scientific Research (C26340039 and B15H02892) from the Japan Society for the Promotion of Science.

References

Chikahisa. L., Oyama, Y., Okazaki, E., Noda, K., 1996. Fluorescent estimation of H_2O_2-induced changes in cell viability and cellular nonprotein thiol level of dissociated rat thymocytes. Jpn. J. Pharmacol. 71, 299–305.

Fracchia, K.M., Pai, C.Y., Walsh, C.M., 2013. Modulation of T cell metabolism and function through calcium signaling. Front. Immunol. 4: 324.

Gee, K.R., Zhou, Z.L., Qian, W.J., Kennedy, R., 2002. Detection and imaging of zinc secretion from pancreatic beta-cells using a new fluorescent zinc indicator. J. Am. Chem. Soc. 124, 776–778.

Harr, M.W., Distelhorst, C.W., 2010. Apoptosis and autophagy: decoding calcium signals that mediate life or death. Cold Spring Harb. Perspect. Biol. 2: a005579

Hedli, C.C., Rao, N.R., Reuhl, K.R., Witmer, C.M., Snyder, R., 1996. Effects of benzene metabolite treatment on granulocytic differentiation and DNA adduct formation in HL-60 cells. Arch. Toxicol. 70, 135–144.

Hiramoto, K., Mochizuki, R., Kikugawa, K., 2001. Generation of hydrogen peroxide from hydroxyhydroquinone and its inhibition by superoxide dismutase. J. Oleo Sci. 50, 21–28.

Kao, J.P., Harootunian, A.T, Tsien, R.Y., 1989. Photochemically generated cytosolic calcium pulses and their detection by fluo-3. J. Biol. Chem. 264, 8179–8184.

Kinazaki A, Sakanashi Y, Oyama TM, Shibagaki H, Yamashita K, Hashimoto E, Nishimura Y, Ishida S, Okano Y, Oyama Y., 2009. Micromolar Zn^{2+} potentiates the cytotoxic action of submicromolar econazole in rat thymocytes: possible disturbance of intracellular Ca^{2+} and Zn^{2+} homeostasis. Toxicol. In Vitro. 23, 610–616.

Koopman, G., Reutelingsperger, C.P., Kuijten, G.A., Keehnen, R.M., Pals, S.T., Van Oers, M.H., 1994. Annexin V for flow cytometric detection of phosphatidylserine expression on B cells undergoing apoptosis. Blood. 84, 1415–1420.

Lee, E.W., Garner, C.D., 1991. Effects of benzene on DNA strand breaks in vivo versus

benzene metabolite-induced DNA strand breaks in vitro in mouse bone marrow cells. Toxicol. Appl. Pharmacol. 108, 497–508.

Lee, E.W., Johnson, J.T., Garner, C.D., 1989. Inhibitory effect of benzene metabolites on nuclear DNA synthesis in bone marrow cells. J. Toxicol. Environ. Health. 26, 277–291.

Lévay, G., Bodell, W.J., 1992. Potentiation of DNA adduct formation in HL-60 cells by combinations of benzene metabolites. Proc. Nati. Acad. Sci. 89, 7105–7109.

Matsui, H., Oyama, T.M., Okano, Y., Hashimoto, E., Kawanai, T., & Oyama, Y., 2010. Low micromolar zinc exerts cytotoxic action under H_2O_2-induced oxidative stress: Excessive increase in intracellular Zn^{2+} concentration. Toxicology. 276, 27–32.

Müller, C., Hofmann, T., 2007. Quantitative studies on the formation of phenol/2-furfurylthiol conjugates in coffee beverages toward the understanding of the molecular mechanisms of coffee aroma staling. J. Agric. Food Chem. 55, 4095–4102.

Müller, C., Hemmersbach, S., van't Slo, G., Hofmann, T., 2006. Synthesis and structure determination of covalent conjugates formed from the sulfury-roasty-smelling 2-furfurylthiol and di- or trihydroxybenzenes and their identification in coffee brew. J. Agric. Food Chem. 54, 10076–10085.

Nishimura, Y., Kanada, A., Yamaguchi, J.Y., Horimoto, K., Kobayashi, M., Tatsuishi, T., Kanemaru, K., Ueno, S., Oyama, Y, 2006. Cytometric analysis of lidocaine-induced cytotoxicity: a model experiment using rat thymocytes. Toxicology. 218, 48–57.

Ochiai, R., Nagao, T., Katsuragi, Y., Tokimitsu, I., Funatsu, K., Nakamura, H., 2008. Effects of hydroxyhydroquinone-reduced coffee in patients with essential hypertension. J. Health Sci. 54, 302–309.

Pellack-Walker, P., Blumer, J.L., 1986. DNA damage in L5178YS cells following exposure to benzene metabolites. Mol. Pharmacol. 30, 42–47.

Robert, V., Triffaux, E., Savignac, M., Pelletier, L., 2011. Calcium signalling in T-lymphocytes. Biochimie. 93, 2087–2094.

Sakanashi, Y., Oyama, K., Matsui, H., Oyama, T.B., Oyama, T.M., Nishimura, Y., Sakai, H., Oyama, Y., 2008. Possible use of quercetin, an antioxidant, for protection of cells suffering from overload of intracellular Ca^{2+}: a model experiment. Life Sci. 83, 164–169.

Sakanashi, Y., Oyama, T.M., Matsuo, Y., Oyama, T.B., Nishimura, Y., Ishida, S., Imai, S., Okano, Y., Oyama, Y., 2009. Zn^{2+}, derived from cell preparation, partly attenuates Ca^{2+}-dependent cell death induced by A23187, calcium ionophore, in rat thymocytes. Toxicol. In Vitro. 23, 338–345.

Schwartz, C.S., Snyder, R., Kalf, G.F., 1984. The inhibition of mitochondrial DNA replication in vitro by the metabolites of benzene, hydroquinone and p-benzoquinone. Chem. Biol. Interact. 53, 327–350.

Suzuki, A., Fujii, A., Jokura, H., Tokimitsu, I., Hase, T., & Saito, I. (2008). Hydroxyhydroquinone interferes with the chlorogenic acid-induced restoration of endothelial function in spontaneously hypertensive rats. Amer. J. Hypertens. 21, 23–27.

Wilson, H.A., Chused, T.M., 1985. Lymphocyte membrane potential and Ca^{2+}-sensitive potassium channels described by oxonol dye fluorescence measurements. J. Cell. Physiol. 125, 72–81.

Figure legends

Figure 1. Effects of hydroxyhydroquinone (HHQ), pyrogalol (PRG), and furaneol (DHF) on cell mortality. Each column and bar indicates the mean value and standard deviation of four to eight samples. Asterisks (**) indicate significant difference ($P < 0.01$) between the control group (CONTROL) and the group of cells treated with the test agent.

Figure 2. Effects of hydroxyhydroquinone (HHQ), pyrogalol (PRG), and furaneol (DHF) on side scatter intensity. (A) Change in the cytogram (forward scatter versus side scatter) induced by HHQ. Each cytogram was constructed with 2500 cells. (B) Effects of HHQ, PRG, and DHF on the mean intensity of the side scatter. Column and bar, respectively, indicate the mean value and standard deviation of four to eight samples. Asterisks (**) indicate significant difference ($P < 0.01$) between the control group (CONTROL) and the group of cells treated with the respective test agents.

Figure 3. Effects of hydroxyhydroquinone (HHQ) in population of cells classified with propidium iodide and annexin V-FITC. (A) Change in cytogram (propidium fluorescence versus FITC fluorescence) of cells incubated with HHQ. Each cytogram was constructed with 2500 cells. N: intact living cells, A: annexin V-positive living cells, P: annexin V-negative dead cells, and AP: annexin V-positive dead cells. (B) Change in the cell population treated with HHQ. Column and bar, respectively, indicate the mean value and standard deviation of four samples. Asterisks (**) indicate significant difference ($P < 0.01$) between the control population (CONTROL) and the population of cells treated with the respective test agents.

Figure 4. Concentration-dependent increase in the intensity of Fluo-3 fluorescence induced by hydroxyhydroquinone (HHQ). Column and bar, respectively, indicate the mean value and

standard deviation of four samples. Asterisks (**) indicate significant difference ($P < 0.01$) between the control group (CONTROL) and the group of cells treated with HHQ.

Figure 5. Effects of external Ca^{2+} removal and $MnCl_2$ on the augmentation of Fluo-3 fluorescence induced by hydroxyhydroquinone (HHQ). (A) HHQ-induced change in Fluo-3 fluorescence under external Ca^{2+}-free conditions. Column and bar, respectively, indicate the mean value and standard deviation of four samples. Asterisks (**) indicate significant difference ($P < 0.01$) between the control group (CONTROL) and the group of cells treated with HHQ under the respective conditions. (B) Effect of $MnCl_2$ on HHQ-induced augmentation of Fluo-3 fluorescence. $MnCl_2$ was applied to the cell suspension after the measurement of Fluo-3 fluorescence from the cells incubated with HHQ for 2 h (Open column). The fluorescence was further measured at 30 min after the application of $MnCl_2$ (Filled column). Asterisks (**) indicate significant difference ($P < 0.01$) between the control group (CONTROL) and the group of cells treated with HHQ. Symbols (##) indicate significant difference ($P < 0.01$) in the intensity of Fluo-3 fluorescence monitored from the cells treated with HHQ in the absence or presence of $MnCl_2$.

Figure 6. Effects of N,N,N′,N′-tetrakis(2-pyridylmethyl)ethylenediamine (TPEN) on the hydroxyhydroquinone (HHQ)-induced augmentation of Fluo-3 and FluoZin-3 fluorescence. (A) HHQ-induced augmentation of Fluo-3 fluorescence in the absence or presence of TPEN. Column and bar, respectively, indicate the mean value and standard deviation of four samples. Asterisks (**) indicate significant difference ($P < 0.01$) between the control group (CONTROL) and the group of cells treated with HHQ. Symbols (##) indicate significant difference ($P < 0.01$) in the intensity of Fluo-3 fluorescence monitored from the cells treated with HHQ in the absence or presence of TPEN. (B) HHQ-induced augmentation of FluoZin-3 fluorescence in the absence or presence of TPEN. Asterisks (**) indicate significant difference ($P < 0.01$) between

the control group (CONTROL) and the group of cells treated with HHQ. Symbols (##) indicate significant difference ($P < 0.01$) in the intensity of FluoZin-3 fluorescence monitored from the cells treated with HHQ in absence or presence of TPEN.

Figure 7. Hydroxyhydroquinone (HHQ)-induced change in the intensity of Oxonol fluorescence. Column and bar, respectively, indicate the mean value and standard deviation of four samples. Asterisks (**) indicate significant difference ($P < 0.01$) between the control group (CONTROL) and the group of cells treated with HHQ.

Figure 1

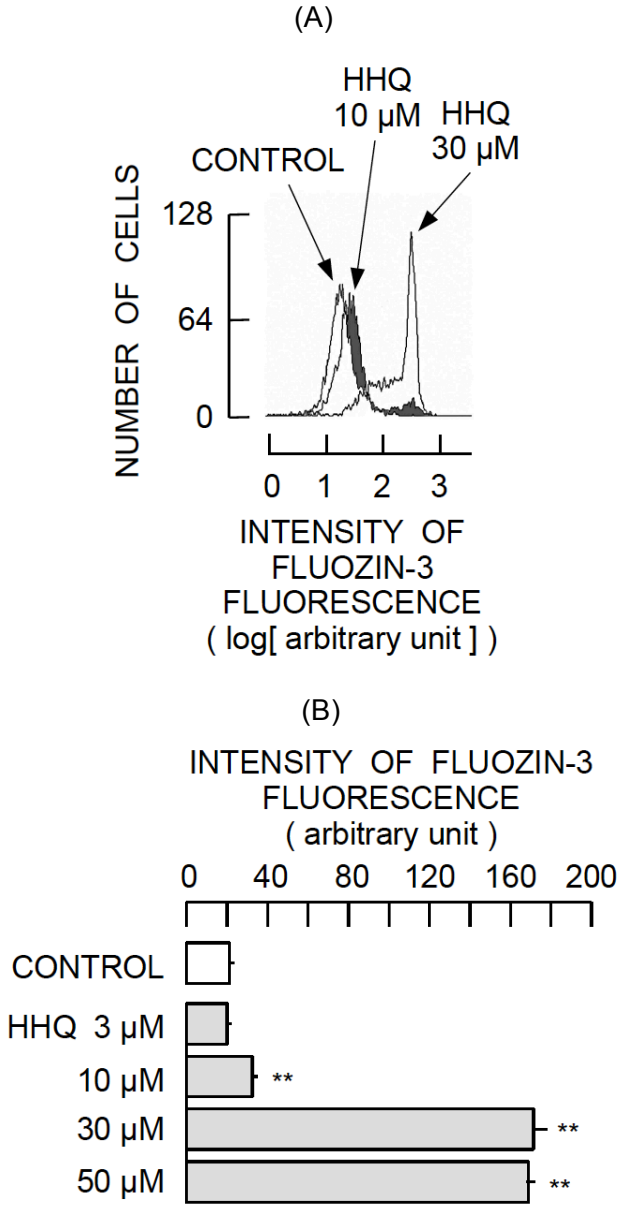
(A)
HHQ
10 μM
HHQ
30 μM
CONTROL
NUMBER OF CELLS
128
64
0
0 1 2 3
INTENSITY OF
FLUOZIN-3
FLUORESCENCE
(log[arbitrary unit])
(B)
INTENSITY OF FLUOZIN-3
FLUORESCENCE
(arbitrary unit)
0 40 80 120 160 200
CONTROL
HHQ 3 μM
10 μM
30 μM
50 μM
**
**
**

Figure 2

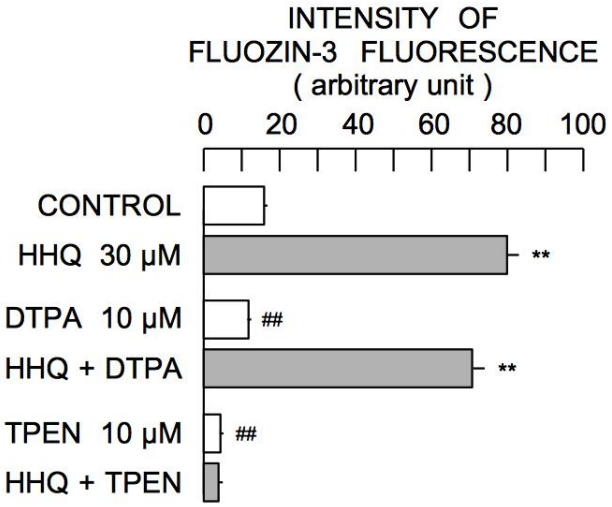
INTENSITY OF
FLUOZIN-3 FLUORESCENCE
(arbitrary unit)
0
20
40
60
80
100
CONTROL
HHQ 30 μM
**
DTPA 10 μM
##
HHQ + DTPA
**
TPEN 10 μM
##
HHQ + TPEN

Figure 3

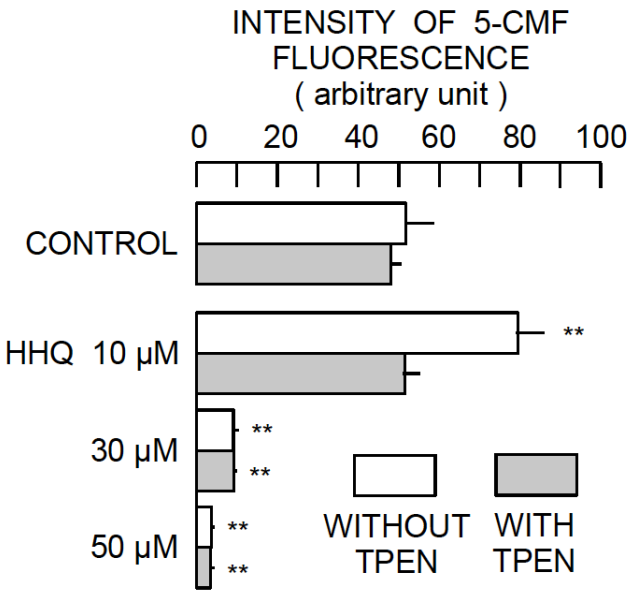
INTENSITY OF 5-CMF
FLUORESCENCE
(arbitrary unit)
0
20
40
60
80
100
CONTROL
HHQ 10 μM
30 μM
50 μM
**
**
**
**
**
WITHOUT
TPEN
WITH
TPEN

Figure 4

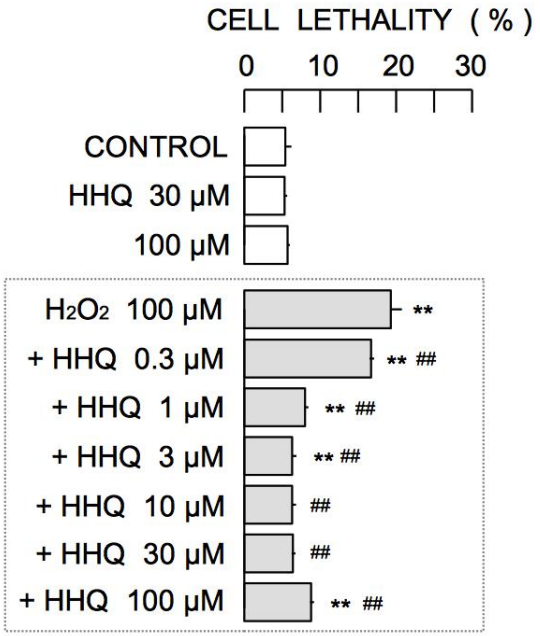
CELL LETHALITY (%)
0
10
20
30
CONTROL
HHQ 30 μM
100 μM
H2O2 100 μM
+ HHQ 0.3 μM
+ HHQ 1 μM
+ HHQ 3 μM
+ HHQ 10 μM
+ HHQ 30 μM
+ HHQ 100 μM
** ##
** ##
** ##
##
##
** ##

Figure 5

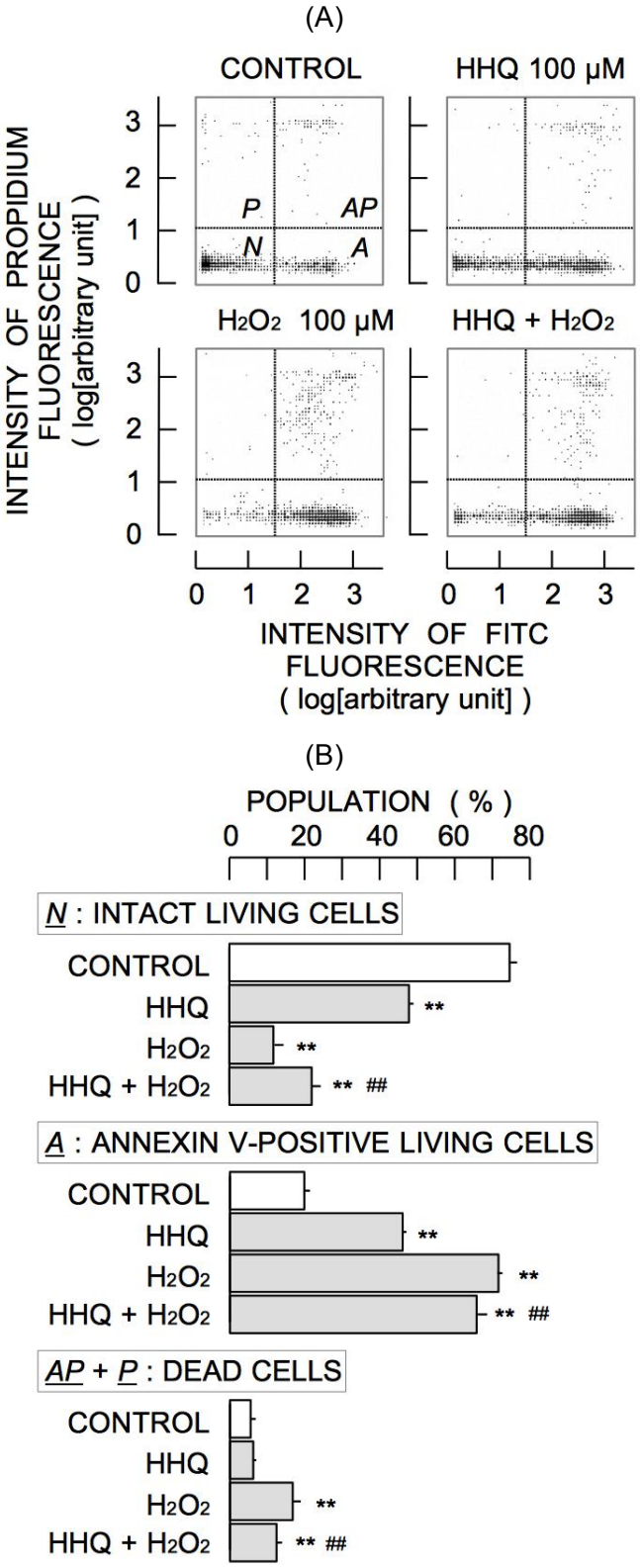
(A)
CONTROL
HHQ 100 μM
H2O2 100 μM
HHQ + H2O2
P
AP
N
A
INTENSITY OF PROPIDIUM FLUORESCENCE (log[arbitrary unit])
INTENSITY OF FITC FLUORESCENCE (log[arbitrary unit])
0 1 2 3
(B)
POPULATION (%)
0 20 40 60 80
N : INTACT LIVING CELLS
A : ANNEXIN V-POSITIVE LIVING CELLS
AP + P : DEAD CELLS
CONTROL
HHQ
H2O2
HHQ + H2O2
** ##

Figure 6

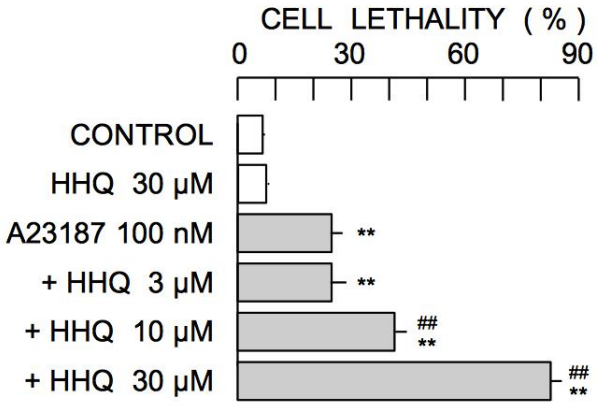
CELL LETHALITY (%)
0
30
60
90
CONTROL
HHQ 30 μM
A23187 100 nM
+ HHQ 3 μM
+ HHQ 10 μM
+ HHQ 30 μM
**
**
##
**
##
**